Peer-reviewed version available at *Molecules* **2018**, *23*, 2960; doi:10.3390/molecules23112960

Article

Membrane-permeable octanoyloxybenzyl-masked cNMPs as novel tools for non-invasive cell assays

Alexandra Ruthenbeck [1], Elisa Marangoni [1,2], Björn-Ph. Diercks [3], Aileen Krüger [3], Viacheslav O. Nikolaev [3], Andreas H. Guse [3] and Chris Meier [1,*]

[1] Organic Chemistry, Department of Chemistry, Faculty of Sciences, University of Hamburg, Martin-Luther-King-Platz 6, D-20146 Hamburg, Germany; chris.meier@chemie.uni-hamburg.de
[2] School of Pharmacy, Medicinal Chemistry Unit, University of Camerino, via S. Agostino 1, 62032 Camerino, Italy,
[3] University Medical Center Hamburg-Eppendorf, Martinistraße 52, 20246 Hamburg, Germany; guse@uke.uni-hamburg.de
* Correspondence: chris.meier@chemie.uni-hamburg.de; Tel.: +49-40-42838-4324

Abstract: Adenine nucleotide (AN) 2nd messengers such as 3′,5′-cyclic adenosine monophosphate (cAMP) are central elements of intracellular signaling, but many details of underlying processes remain still elusive. Like all nucleotides, cyclic nucleotide monophosphates (cNMPs) are net-negatively charged at physiologic pH which limits their applicability in cell-based settings. Thus, many cellular assays rely on sophisticated techniques like microinjection or electroporation. This setup is not feasible for medium- to high-throughput formats, and the mechanic stress that cells are exposed to raises the probability of interfering artefacts or false-positives.
Here, we present a short and flexible chemical route yielding membrane-permeable, bio-reversibly masked cNMPs for which we employed the octanoyloxybenzyl (OB) group. We further show hydrolysis studies on chemical stability and enzymatic activation, and present results of real-time assays, where we used cAMP and Ca^{2+} live cell imaging to demonstrate high permeability and prompt intracellular conversion of some selected masked cNMPs. Consequently, our novel OB-masked cNMPs constitute valuable precursor-tools for non-invasive studies on intracellular signaling.

Keywords: cyclic nucleotide monophosphate; bio-reversible protection; acyloxybenzyl phosphate ester.

1. Introduction

Among cNMPs, the ubiquitous second messengers cAMP and cGMP constitute the most prominent examples but also 'non-canonical' cNMPs such as 3′,5′-cyclic uridine monophosphate (cUMP) have been reported and related to signaling processes.[1] For example, cAMP plays an important role in many biological processes, in addition to its implication in Ca^{2+} mobilization. This cyclic mononucleotide is generated from ATP through G protein-coupled receptor (GPCR) based activation of adenylyl cyclase (AC). The signaling by cNMPs proceeds via two general pathways. The first relies on direct binding and regulation of distinctive cyclic nucleotide-gated (CNG) ion channels. The second mechanism is based on the activation of protein kinases A (PKA) or G to further transduce the signal.[1–4]

Activated PKA/G promotes phosphorylation of a variety of proteins, which can be involved in the regulation of metabolic processes, muscle contraction and gene transcription.[4] In contrast, signaling through CNG channels allows a faster processing and implementation of increased cNMP levels. The ion channels are generally non-selective for cations. However, the entry of sodium ions (Na^{+}) depolarizes the membrane which promotes the combined influx of Ca^{2+}. Additionally, voltage-gated Ca^{2+} channels open in response to membrane depolarization and thus enhance the

Peer-reviewed version available at Molecules 2018, 23, 2960; doi:10.3390/molecules23112960

Ca^{2+} signal further.[2,3] Signals of cAMP and cGMP are ceased through their degradation by phosphodiesterase to AMP and GMP, respectively.[2,3]

Due to the ubiquitous involvement in cellular processes, the role of cNMP signaling in the context of inflammation and regulation of immune response constitutes a research field of rising interest. It was for example found that regulatory T cells (T_{reg}) exert their suppressive effect on effector T cells (T_{eff}) through increasing concentrations of cAMP. The rise of cAMP levels in T_{eff} could either be induced via a paracrine mechanism, or by a direct transfer of cAMP via gap junctions between T_{reg} and T_{eff}.[5,6] However, the transfer of cAMP between a pair of T cells could not be visualized directly yet, and also the underlying mechanisms allowing T_{reg} cells to produce such significantly higher cAMP levels than T_{eff} cells are not elucidated to date. A loss of this immuno-suppressive mechanism could contribute to the generation of autoimmune reactions. Understanding the role of cNMPs in inflammation and T cell regulation and identifying the associated molecular pathways thus could enable the identification of novel targets in the treatment of autoimmune disease.

Cell-based studies on 2nd messengers are generally difficult to perform as application of the highly polar compounds is carried out via effortful, single-cell preparative methods like electroporation, microinjection or patch clamp. These methods require highly trained staff, careful preparation and significant amounts of time in advance of each experiment while at the same time the invasive application raises the potential for interfering artefacts or false-positives.[7] Membrane permeable, bio-reversibly modified chemical derivatives of second messengers are highly desirable to circumvent this drawback.

First reports on protected cNMPs by Engels *et al.* included cAMP and cGMP derivatives carrying different benzyl groups at the phosphate.[8,9] Hughes *et al.* reported the synthesis and biologic evaluation of N^6,O^2-dibutyryl cAMP-acetoxymethyl (AM) ester.[10] The synthesis started from N^6,$O^{2'}$-dibutyryl cAMP, which was converted with AM bromide (AM-Br) under DIEA-basic conditions in CH_3CN over 4 days at room temperature.[10] The obtained masked nucleotide was used in whole-cell incubation studies where an activation of PKA proceeded, but only 15 min after the addition of di(Bu)cAMP-AM (10 µM) to the cell medium.[10] In a further study, Schultz *et al.* synthesized cAMP-AM via a transient protection of the 2'-OH function with the trimethylsilyl (TMS) group and successive esterification of the phosphate under the before described conditions.[11] Despite a PKA activating effect of cAMP-AM the researchers found that cAMP-AM was less potent than di(Bu)cAMP-AM and metabolized so rapidly that it gave only transient signals.[11] The synthesis of AM-esters of cCMP and cUMP have also been reported.[12] However, cNMP-AMs are not applicable for all cell types, seemingly due to insufficient chemical stability, and flexibility of the synthesis approach is limited by availability of the respective cNMP.

The acyloxybenzyl (AB)-masking system was introduced originally for nucleoside monophosphate (NMP) prodrugs and successfully transferred on nucleoside diphosphates (NDPs) and nucleoside triphosphates (NTPs).[13–17] The respective prodrugs were shown to efficiently diffuse across cell membranes and release the corresponding nucleotide intracellularly upon enzymatic activation.[14] Further, the concept was expanded on compound classes like sugar nucleotides.[18] The broad synthetic applicability of the AB masking group is complimented by meeting the essential features of a prodrug concept: i) high chemical stability, ii) efficient enzymatic activation and iii) sufficient lipophilicity to enable the passage through cell membranes. Moreover, the two-part composition of the AB-masks allows variation of e.g lipophilicity or enzymatic cleavability which adds further versatility to the concept.[13–15,19–21] Consequently, the AB-concept was investigated for expansion on cNMPs to provide tools for studies on cellular effects like e.g. calcium signaling in bulk settings on a variety of cells and without the need for example of microinjection. As a first example, an octanoyloxybenzyl (OB)-mask was used here.

2. Results and Discussion

Inspiration for the synthesis approach towards OB-masked cNMPs was drawn from own studies on the synthesis of non-symmetric phosphoramidites (PAs) that included an unprotected nucleoside moiety. In these cases, side reactions were repeatedly observed amongst which the formation of phosphites was prominent. These phosphites were concluded to result either from an intermolecular or an intramolecular substitution of the remaining *N*-di*iso*propyl group by a second nucleosidic hydroxy-group. In the latter case, a cyclic nucleoside phosphite would constitute the reaction product, and further oxidation would result in a cyclic nucleoside monophosphate derivative.

Based on this hypothesis, we set up a synthesis involving different nucleosides and an OB-masked phosphordiamidite (OBPA$_2$).

2.1. Preparation of AB-masked cNMPs

2.1.1. Synthesis of starting materials

The synthesis of bis(*N*,*N*-di*iso*propylamino)-4-octanoyloxybenzyl phosphordiamidite (OBPA$_2$) was adapted from Weinschenk *et al.* who used the building block for the synthesis of non-symmetric PAs.[22] The reaction was performed as described in the literature starting from bis(*N*,*N*-di*iso*propylamino)chlorophosphine **1** and 4-(hydroxymethyl)phenyloctanoate **2**, and yielded OBPA$_2$ **3** in 71% (Scheme 1).

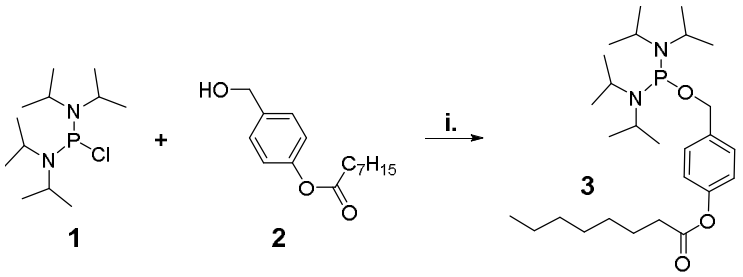

Scheme 1. Synthesis of OBPA$_2$ **3**: (**i.**) 1 equiv. **1**, 1 equiv. **2**, 1.3 equiv. TEA, THF, rt, 18 h, **3**: 71%.

The nucleosides adenosine (A, **4**), 2'-deoxy adenosine (dA, **5**) and guanosine (G, **6**) were mono-*N*-butyrylated to add further lipophilicity to the envisaged OB-cNMPs. N^6-Butanoyl-adenosine **7** was synthesized starting from adenosine **4** via transient silylation of all hydroxy-groups to selectively introduce the butyryl moiety at the N^6-position.[23] The desired protected nucleoside **7** was obtained in 61% yield after automated RP flash column chromatography (Figure 2). The yield was limited by the formation of *N*,*N*-diacylated adenosine and partial cleavage of the glycosidic bond during concentration of the crude reaction mixture. Analogously, N^6-butanoyl-dA **8** and N^2-butanoyl-G **9** were synthesized starting from the respective nucleosides and obtained in yields of 32% and 48%, respectively (Scheme 2).

2.1.2. Syntheses of OB-cNMPs

First, a model system, as which the route towards octanoyloxybenzyl-masked cUMP (OB-cUMP, **10**) served, was set up to study course and outcome of the phosphitylation in more detail.

The starting conditions for the synthesis of OB-cUMP **10** were adapted from the approaches towards non-symmetric PAs.[22] 4,5-Dicyanoimidazole (DCI, 0.25 M in CH_3CN) was used as activator for the PA-coupling, and *t*BuOOH (5.5 M in n-decane) served as oxidizing agent. The reaction was carried out in a mixture of acetonitrile and DMF due to the limited solubility of uridine **11** in CH_3CN (Scheme 3).

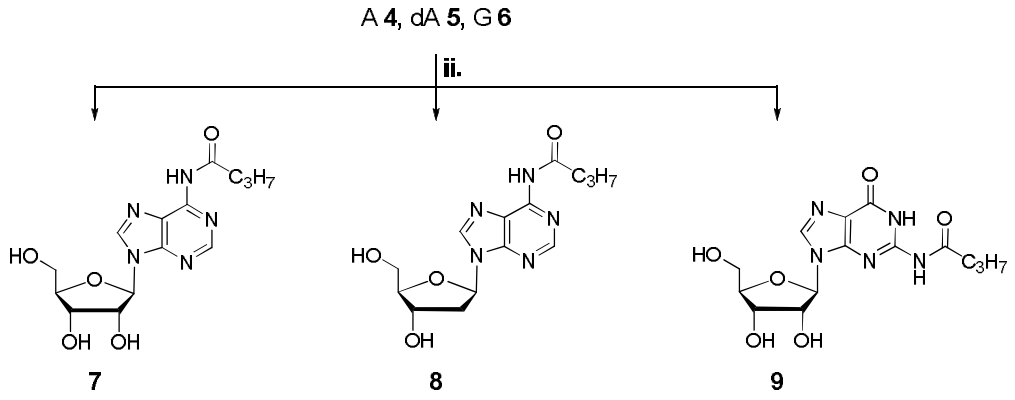

Scheme 2. Synthesis of *N*-butyryl nucleosides **7**-**9**: (**ii.**) first 2.1 - 9.0 equiv. TMSCl, 0 °C to rt, 18 h, second 1.1 equiv. butanoyl chloride, pyridine/THF or pyridine/CH_2Cl_2, rt, 5 - 18 h, third 1 M aq. HCl or CH_3OH, rt, 5 min or 18 h, **7**: 61%, **8**: 32%, **9**: 48%.

In the first attempt, a solution of nucleoside **11** and $OBPA_2$ **3** was treated with 2.2 equivalents of DCI that were added dropwise at 0 °C. The reaction mixture was allowed to warm to rt and stirred 30 min more before *t*BuOOH was added for oxidation. Lastly, the crude reaction mixture was purified by automated RP flash column chromatography, and the masked cyclic nucleotide **10** was obtained as a mixture of two diastereomers in a yield of only 13 % (Scheme 3).

Prompted by the surprisingly low yield, the reaction course was studied ^{31}P-NMR spectroscopically (Fig. 1). Interestingly, upon just mixing uridine **11** and $OBPA_2$ **3**, the diamidite was converted almost quantitatively and a signal at 13.2 ppm formed (Fig. 1). Comparison with literature-data indicated that this signal likely corresponded to an activated amidite.[24] Furthermore, signals in the range of PAs and phosphites were formed already as well (Fig. 1, top). The addition of DCI then promoted the formation of the intermediate PA, but formation of the anticipated cyclic phosphite seemed to occur only at low proportion. Steric hindrance in the attack of the 3′-hydroxy group on the phosphorous atom or an insufficient nucleophilicity may be the reasons that led to an insufficient formation of the cyclic phosphite.

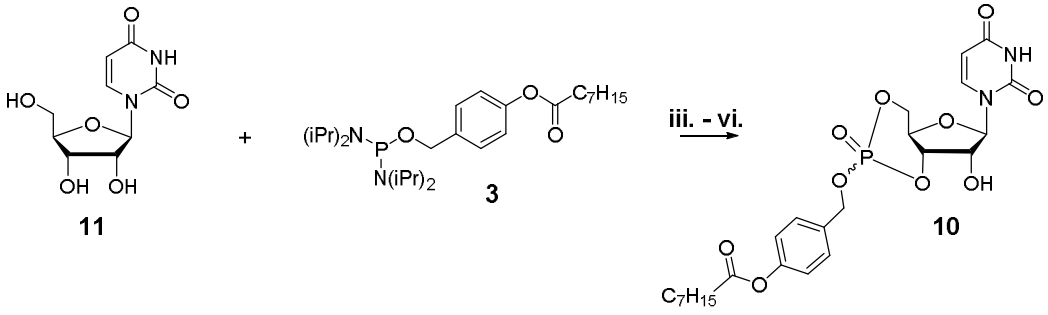

Scheme 3: (**iii.**) 1.1 equiv. **3**, 2.2 equiv. DCI (0.25 M in CH_3CN), 1.5 equiv. *t*BuOOH (5.5 M in *n*-decane), CH_3CN/DMF 5:4, 0 °C to rt, 60 min, **10**: 13%. (**iv.**) 1.1 equiv. **3**, first portion of 1.3 equiv. DCI (0.25 M in CH_3CN), second portion of 1.3 equiv. DCI (0.25 M in CH_3CN), 1.5 equiv. *t*BuOOH (5.5 M in *n*-decane), CH_3CN/DMF 5:1, rt, 60 min, **10**: 15%. (**v.**) 1.1 equiv. **3**, first portion of 1.3 equiv. DCI (0.25 M in CH_3CN), second portion of 1.3 equiv. BTT (0.3 M in CH_3CN), 1.5 equiv. *t*BuOOH (5.5 M in *n*-decane), CH_3CN/DMF 5:1, rt, 60 min, **10**: 13 – 19%. (**vi.**) 1 – 1.2 equiv. **3**, first portion of 1 – 1.2 equiv. saccharin and 1 – 1.2 equiv. 1-methylimidazole, second portion of 1 – 1.2 equiv. saccharin and 1 – 1.2 equiv. 1-methylimidazole, 1.5 equiv. *t*BuOOH (5.5 M in *n*-decane), CH_3CN/DMF 5:1, rt, 60 min to 72 h, **10**: 16 – 19%.

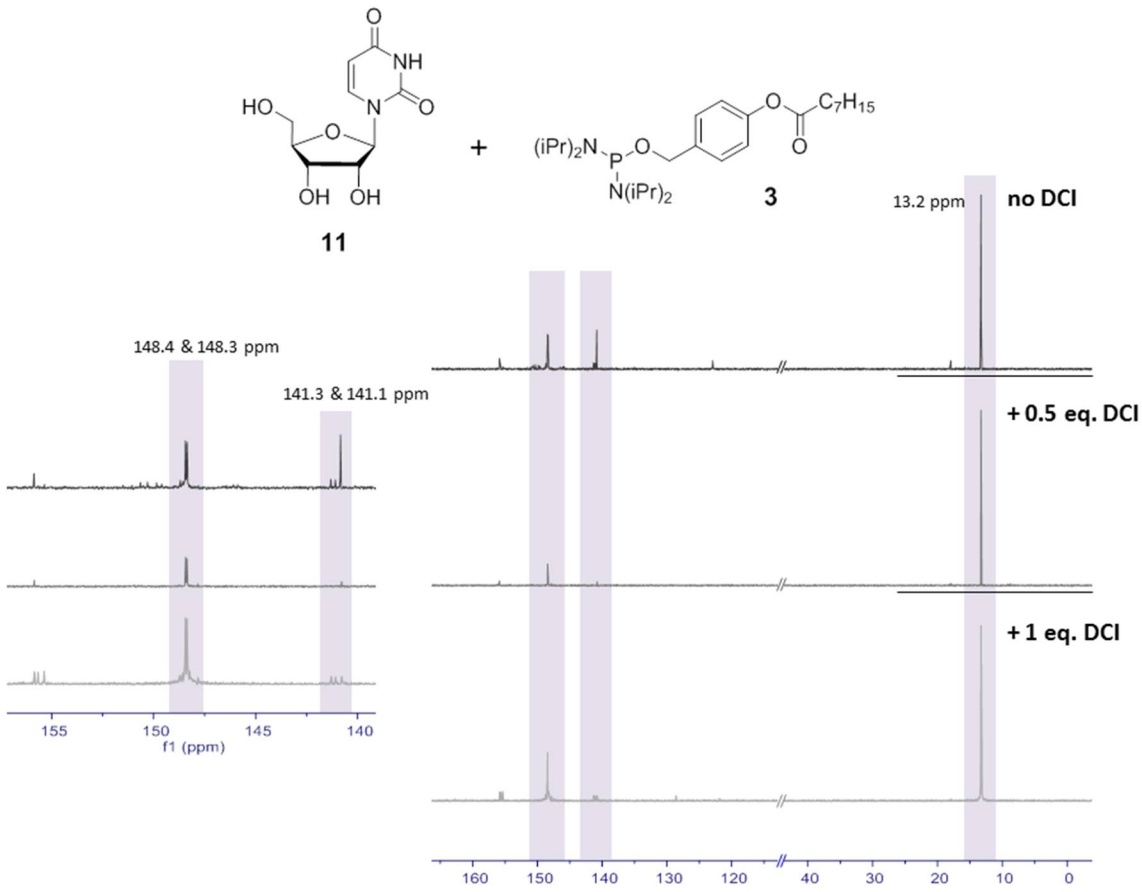

Figure 1: ^{31}P-NMR spectra (CH_3CN-d_3, 162 MHz, 25 °C, shifts δ in [ppm]) of the reaction monitoring between uridine **11** and $OBPA_2$ **3**.

The synthesis of OB-cUMP **10** consequently was repeated with several changes to the protocol in order to evaluate the influence of the reaction conditions and in particular the impact of the activator (Scheme 3).

In a second approach, the ratio between CH_3CN and DMF was altered to 5:1 and the mode of addition of reagents was changed. This time, the nucleoside was placed in the reaction flask and dissolved in CH_3CN/DMF 5:1. A separate solution of $OBPA_2$ **3** in CH_3CN and one equivalent of DCI were added slowly and dropwise to nucleoside **11** at rt. Once the addition was completed, a second equivalent of DCI was added, and the reaction mixture stirred at rt for 60 min. After the successive oxidation and final purification, OB-cUMP **10** was obtained in 15% yield. Consequently, the outcome of the reaction was almost identical to that of the attempt before.

Next, the activator was changed to 5-(benzylthio)-1*H*-tetrazole (BTT) which displays a higher acidity and lower nucleophilicity than DCI, and the reaction protocol was varied as follows: uridine **11** was dissolved in CH_3CN/DMF 5:1 and successively treated with a solution of $OBPA_2$ **3** in CH_3CN and one equivalent DCI. Both reagents were added in small portions over a period of 30 min. Upon completed addition, the reaction mixture was stirred another 30 to 120 min at rt. Then, one equivalent BTT was added slowly and dropwise over 10 min, and the reaction was kept stirring for further 15 to 60 min. After the subsequent oxidation and final purification, OB-cUMP **10** was isolated in yields between 13 – 19% which again constituted no significant improvement of the reaction outcome. Lastly, an alternative activator-system composed of saccharine and 1-methylimidazole was tested as it was reported to efficiently mediate also reactions between PAs and poorly nucleophilic alcohols like tertiary alcohols.[25]

Saccharine and 1-methylimidazole were dissolved in a 1:1 ratio in CH_3CN prior to the reaction to generate the activating salt. Simultaneously with $OBPA_2$ **3**, one equivalent of the activator salt was

Preprints (www.preprints.org) | NOT PEER-REVIEWED | Posted: 12 October 2018 doi:10.20944/preprints201810.0266.v1

Peer-reviewed version available at Molecules 2018, 23, 2960; doi:10.3390/molecules23112960

added to a solution of uridine **11** in CH_3CN/DMF 5:1. Upon completion of the first addition, the reaction mixture was stirred for 30 min, then treated with a second equivalent of the activator solution and successively stirred for another 60 min to 72 h. After oxidation and automated RP column chromatography, the desired product **10** was obtained in yields between 16 – 19%. Monitoring of the reaction course via ^{31}P-NMR spectroscopy indicated an incomplete activation of OBPA$_2$ **3** even after 72 h. Further, the activated intermediates were again not converted efficiently to the desired phosphite as concluded from the persistence of the respectively attributed phosphorous signals.[25] This alternative approach constituted thus no improvement in comparison to the previous protocols neither. In summary, the isolation of OB-cUMP **10** succeeded repeatedly despite low yields, and thus the reaction protocols were transferred on the *N*-butyrylated nucleosides **7** – **9** (Scheme 4).

The *N*-butyrylated OB-cNMPs **12**–**14** were prepared following the synthesis protocols **iv.** and **v.** described above. The yields obtained for OB-*N*(Bu)-cAMP **12** and OB-*N*(Bu)-cdAMP **13** were in a similar range as found for OB-cUMP **10** with 14% and 13%, respectively (Scheme 4). The reaction towards OB-*N*(Bu)-cGMP **14** proceeded to a lower extent and accordingly, the desired product was isolated in a comparably low yield of 4% (Scheme 4). Interestingly, in the case of **14** the formation of only one of the two possible diastereomers seemed favored as crude ^{31}P-NMR spectra indicated. Here, only one of the possible two phosphate signals was prominent, and consequently, OB-*N*(Bu)-cGMP **14** was isolated as a single diastereomer. Additionally to the *N*-acylated derivative **12**, the NH_2-unmodified OB-cAMP **15** was prepared. The synthesis was performed analogously to OB-cUMP **10** starting from nucleoside **4** and following synthesis variant iii. which made use of a stepwise addition of the in total applied 2.4 equivalents DCI (Scheme 5).

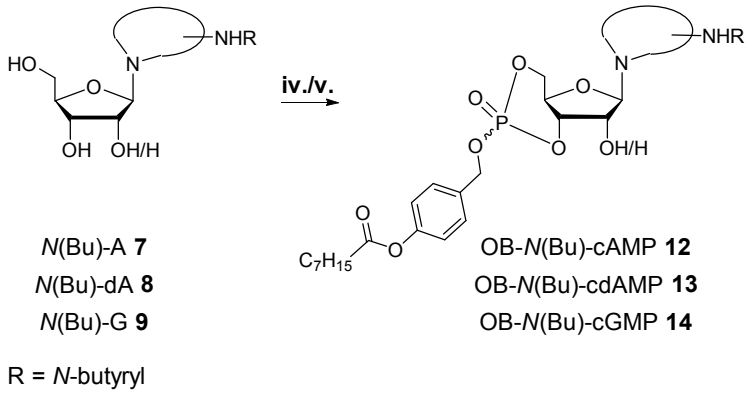

Scheme 4: Syntheses of and *N*-butyrylated OB-cNMPs **12**–**14**: to **12**: (**v.**) 1.1 equiv. **3**, first portion of 1.3 equiv. DCI (0.25 M in CH_3CN), second portion of 1.3 equiv. BTT (0.3 M in CH_3CN), 1.5 equiv. *t*BuOOH (5.5 M in *n*-decane), CH_3CN/DMF 3:1, rt, 60 min, **12**: 14%. To **13**: (**iv.**) 1.1 equiv. **3**, first portion of 1.3 equiv. DCI (0.25 M in CH_3CN), second portion of 1.3 equiv. DCI (0.25 M in CH_3CN), 1.5 equiv. *t*BuOOH (5.5 M in *n*-decane), CH_3CN/DMF 1:1, rt, 60 min, **13**: 13%. To **14**: (**iv.**) 1.1 equiv. **3**, first portion of 1.5 equiv. DCI (0.25 M in CH_3CN), second portion of 1.5 equiv. DCI (0.25 M in CH_3CN), 1.5 equiv. *t*BuOOH (5.5 M in *n*-decane), CH_3CN/DMF 1:1, rt, 60 min, **14**: 4%.

In summary, five different OB-cNMPs were successfully synthesized. With regard to the overall similar outcomes of the various preparations, the scope of the reaction can likely be expanded on further nucleosides and/or differently masked PA$_2$s. This makes the chosen approach individually adaptable and very flexible, particularly in contrast to the previously reported procedures involving AM esters.

Concluding the syntheses, the functional evaluation of selected OB-cNMPs was performed next.

Preprints (www.preprints.org) | NOT PEER-REVIEWED | Posted: 12 October 2018 doi:10.20944/preprints201810.0266.v1

Peer-reviewed version available at Molecules 2018, 23, 2960; doi:10.3390/molecules23112960

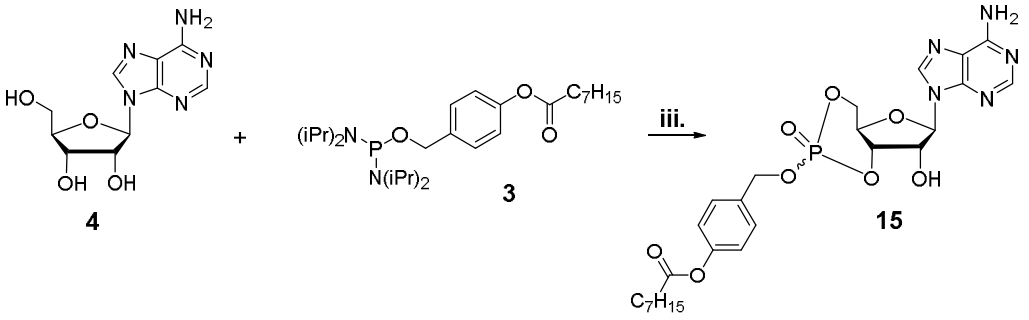

Scheme 5: Preparation of OB-cAMP **15**: **iii.** 1.1 equiv. **3**, 2.4 equiv. DCI (0.25 M in CH_3CN) added in two portions, 1.5 equiv. *t*BuOOH (5.5 M in *n*-decane), CH_3CN/DMF 1:1, rt, 60 min, **15**: 12%.

2.2. Functional evaluation of selected OB-cNMPs

Ideally, masked precursors of bio-active compounds are biologically inactive and display a stability in physiologic media that on the one hand exceeds their specific activation significantly, and on the other hand guarantees sufficient time for their approximation to their respective target structure. Once activated, the previously inactive compound regains its biologic activity back and should accordingly displays respective effects from target interaction. These demands applied for the prepared OB-cNMPs equally as e.g. for nucleotide prodrugs. Consequently, the chemical stability of the OB-cNMPs under physiologic conditions as well as the efficiency of the enzymatic activation of the OB-mask by an exemplary esterase was evaluated. In complementation, the masked nucleotides were applied in various cell assays to analyze their biologic effects e.g. in the context of Ca^{2+} mobilization and cell activation.

2.2.1. Investigation of chemical stability and enzymatic activation by PLE

Stability determinations for OB-cNMPs **10**,**12** and **13** (as 5 mM stock sol. in DMSO) were performed in PBS (50 mM, pH 7.3) as physiologic pH mimic. The compounds (2 mM, final conc. in PBS/DMSO) were incubated over 120 to 200 h at 37 °C. Hydrolysis samples were taken at distinctive times and analyzed via HPLC/MS (Fig. 2 & 3). The recorded HPLC chromatograms and ESI mass spectra showed that the OB-cNMPs released only their respective parent cNMP from cleavage of the OB-mask without the formation of further cleavage byproducts (Fig. 3).

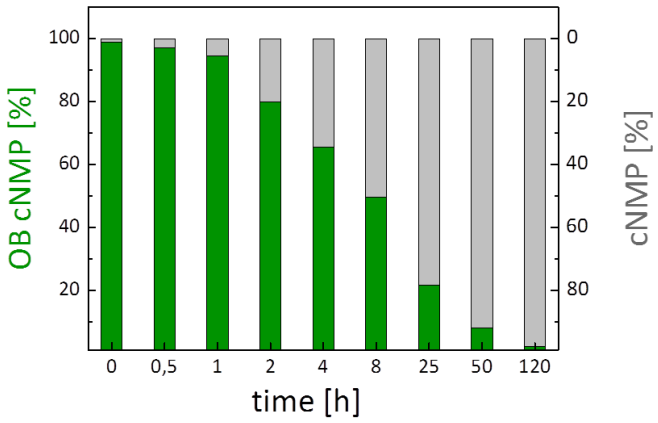

Figure 2: Course of the chemical hydrolysis of OB-*N*(Bu)-cAMP **12** to *N*(Bu)-cAMP **15** given as normalized values for each time point analyzed. Similar hydrolysis courses were measured for OB-cNMPs **10** and **13**.

Preprints (www.preprints.org) | NOT PEER-REVIEWED | Posted: 12 October 2018 doi:10.20944/preprints201810.0266.v1

Peer-reviewed version available at Molecules 2018, 23, 2960; doi:10.3390/molecules23112960

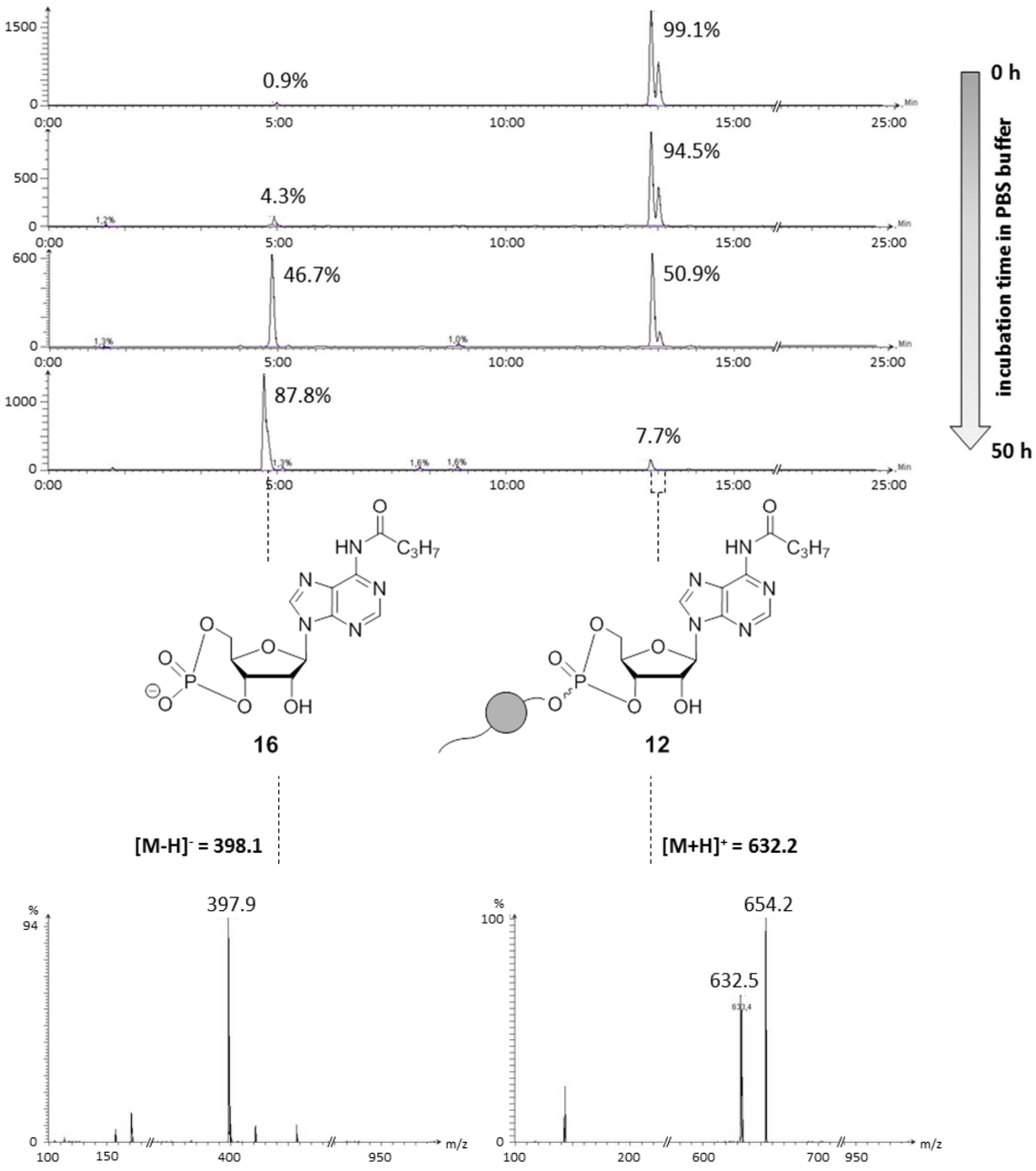

Figure 3: HPLC chromatograms and ESI mass spectra of the chemical hydrolysis of OB-*N*(Bu)-cAMP **12** in PBS (50 mM, pH 7.3) at 0 h, 1 h, 8 h & 50 h. The two signals of the diastereomers vanished over time while the signal for *N*(Bu)-cAMP **15** increased. The compounds were assigned from the mass spectra recorded at the retention times coinciding with the signals found in the HPLC chromatograms.

It was found that after approximately 8 h 50% of the OB-cNMPs were hydrolyzed (**10**: $t_{½}$ = 8.6 h, **12**: $t_{½}$ = 7.4 h, **13**: $t_{½}$ = 7.5 h) (Fig. 2). This half-life implied a stability of the OB-cNMPs that should facilitate convenient setups of cell-based assays and allow for satisfactory time to run, for example, even (pre-) incubation experiments with the masked nucleotides.

The hydrolysis behavior of **10**,**12** and **13** was assessed further, and the relative areas of signals for OB-cNMP and cNMP were determined (in percent). These values were normalized and then averaged for all three hydrolyses under determination of their standard deviation. By this procedure, the individual hydrolysis courses were compared with another since the progress of

Preprints (www.preprints.org) | NOT PEER-REVIEWED | Posted: 12 October 2018 doi:10.20944/preprints201810.0266.v1

Peer-reviewed version available at Molecules 2018, 23, 2960; doi:10.3390/molecules23112960

hydrolyses was expected to be largely similar as the dissociation of the OB-mask should constitute the determinant process.

The average deviation of the hydrolysis progress for OB-cNMPs **10**,**12** and **13** at the time points measured was 5% with a single value maximum of 12%. From these calculations, it was deduced that the hydrolysis course was indeed analog for all OB-cNMPs tested and subject to the pace of the cleavage of the masking group and was almost independent of the nucleotide employed.

After successful probing the chemical stability of the OB-cNMPs satisfying, their enzymatic activation by pig liver esterase (PLE) as an exemplary esterase was evaluated. The incubations of OB-cNMPs **10**,**12** and **13** (2 mM final conc. in PBS/DMSO) with PLE were carried out with 0.05 u PLE per hydrolysis sample (V = 20 µL) which enabled good traceability of the enzymatic conversion (Fig. 4). Again, no further cleavage products apart from the respective cNMPs were determined. The *N*-butyryl group of **12** and **13** was not cleaved by PLE, even at longer incubation times (up to 60 min), as expected. The acquired chromatograms were processed as described for the chemical hydrolysis to compare the progresses of the individual incubations with PLE (Fig. 5). The half-lives of the studied OB-cNMPs were around 5 min under the applied conditions, which, however depended significantly on the amount of esterase present. More importantly in this context, the enzymatic activation of OB-cNMPs proceeded even at low PLE concentrations significantly faster than their decomposition in PBS by a factor of approximately 100. In addition, the enzymatic hydrolyses showed analog progression as indicated by a mean deviation of normalized signal areas for OB-cNMPs and cNMPs of 4% with a maximum deviation of 9% for single time point values (Fig. 5). This permitted again the conclusion that the enzymatic reaction was almost independent of the type of nucleotide and relied on the OB-mask applied.

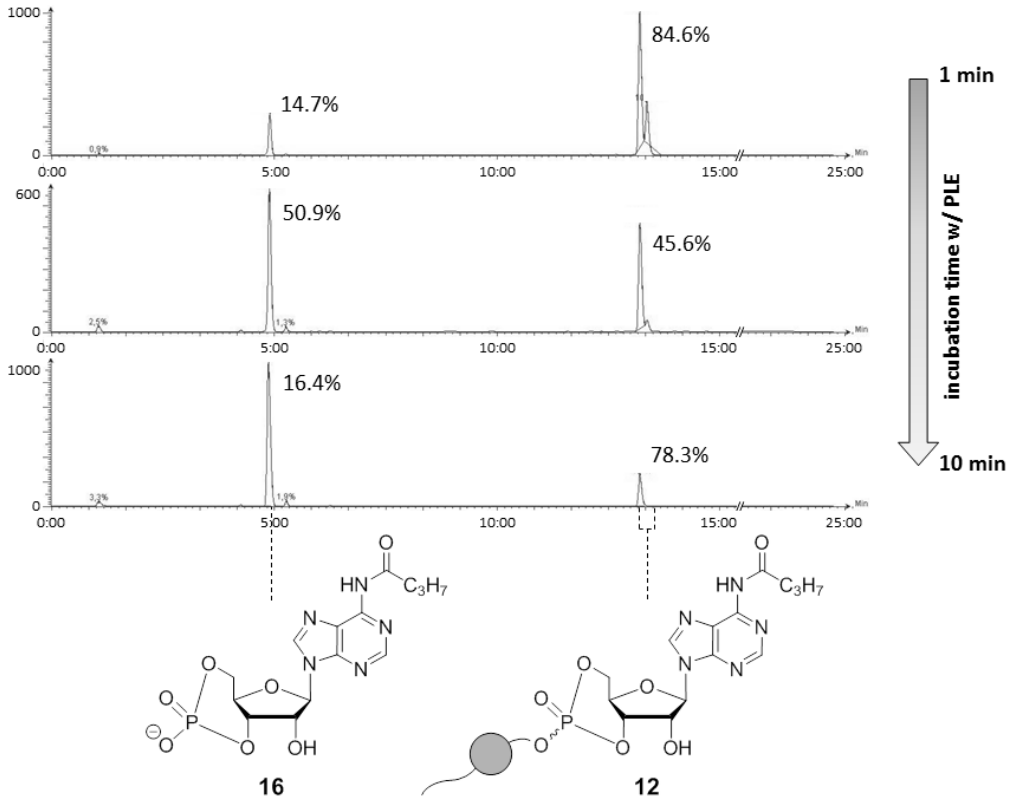

Figure 4: HPLC chromatograms and ESI mass spectra of the enzymatic hydrolysis of OB-*N*(Bu)-cAMP **12** in with PLE (0.05 u/hydrol. sol.) in PBS (50 mM, pH 7.3) at 1, 5 & 10 min. The two signals of the diastereomers vanished over time while the signal for *N*(Bu)-cAMP **15** increased. The compounds were assigned from mass spectra recorded at the retention times coinciding with the signals found in the HPLC chromatograms.

Peer-reviewed version available at Molecules 2018, 23, 2960; doi:10.3390/molecules23112960

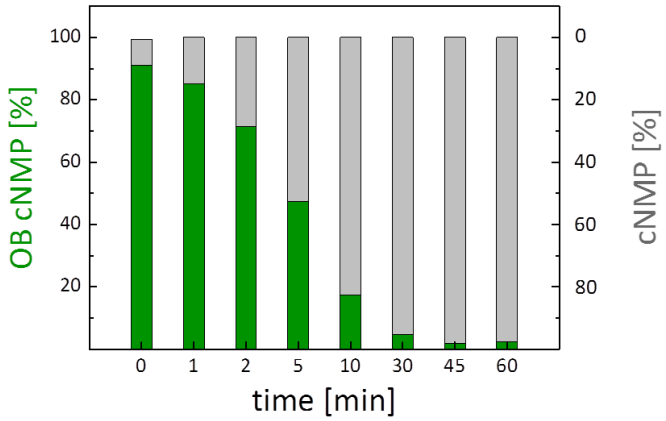

Figure 5: Course of the enzymatic hydrolyses of of OB-*N*(Bu)-cAMP **12** to *N*(Bu)-cAMP **15** given as normalized values for each time point analyzed. Similar hydrolysis courses were measured for OB-cNMPs **10** and **13**.

In summary, the results of both hydrolysis studies, chemical and enzymatic, went well along with the initial criteria as they showed that the stability of the prepared OB-cNMPs was significantly higher than the rate of enzymatic activation. Further, the masked nucleotides proved to be satisfactory stable for application in cell-based assays as their stabilities allow for incubations even over several hours.

Encouraged by the promising hydrolysis properties, the ability of the OB-cNMPs to cross cellular membranes as well as their potential to induce cellular processes was studied successively.

2.2.2. Performance of selected OB-cNMPs in cell-based settings

Primary mouse cardiomyocytes carrying a FRET-sensor with a cAMP binding site were used to examine the membrane-permeability of OB-*N*(Bu)-cAMP **12** in particular. The binding of intracellular cAMP to the FRET sensor is indicated by a decreasing FRET-signal and an increasing fluorescence ratio between cyan-fluorescent protein (CFP) and yellow-fluorescent protein (YFP).[26] FRET-sensor carrying mouse cardiomyocytes were incubated with OB-*N*(Bu)-cAMP **12** (20 mM, at t ≈ 60 s) (Fig. 6). Immediately after addition of **12** to the extracellular medium, the ratio between CFP and YFP started to increase and reached a steady maximum state at circa 110 s. These results imply that OB-*N*(Bu)-cAMP **12** instantaneously crossed the cell membrane and was also rapidly activated by intracellular esterases. Further, the product of the activation process was successfully recognized by the cAMP binding site of the FRET sensor. For the studied substrate, OB-*N*(Bu)-cAMP **12**, this implicated that the N^6-butyryl group was either removed by enzymatic hydrolysis, or that its presence had no detrimental effect on receptor interaction.

In a second setup, Jurkat T cells were loaded with the Ca^{2+}-sensitive fluorescent dye Fura-2. Upon intracellular elevation of Ca^{2+}, the absorption ratio between the two excitation wavelengths of Fura-2 at 340 nm and 380 nm increases. This effect correlates directly with the amount of free cytosolic Ca^{2+}. Jurkat T cells loaded with Fura-2 were stimulated with OB-cNMPs **10**, **12** and **13** (20 µM in DMSO, at t ≈ 120 s) added to their extracellular medium (Fig. 7). The Fura-2 ratio rose rapidly almost immediately after addition of OB-*N*(Bu)-cAMP **12**, and reached its maximum after approximately 200 s. Then, the Ca^{2+} signal slowly decreased as indicated by the degression of the signal. A similar trend was observed for OB-cUMP **10** but the induced Ca^{2+} signal was significantly reduced compared to **12** (Fig. 7). In the case of OB-*N*(Bu)-cdAMP **13**, no initial increase of the intracellular Ca^{2+} concentration was measured. However, the ratio seemed to increase slightly over time (Fig. 7).

Preprints (www.preprints.org) | NOT PEER-REVIEWED | Posted: 12 October 2018 doi:10.20944/preprints201810.0266.v1

Peer-reviewed version available at Molecules 2018, 23, 2960; doi:10.3390/molecules23112960

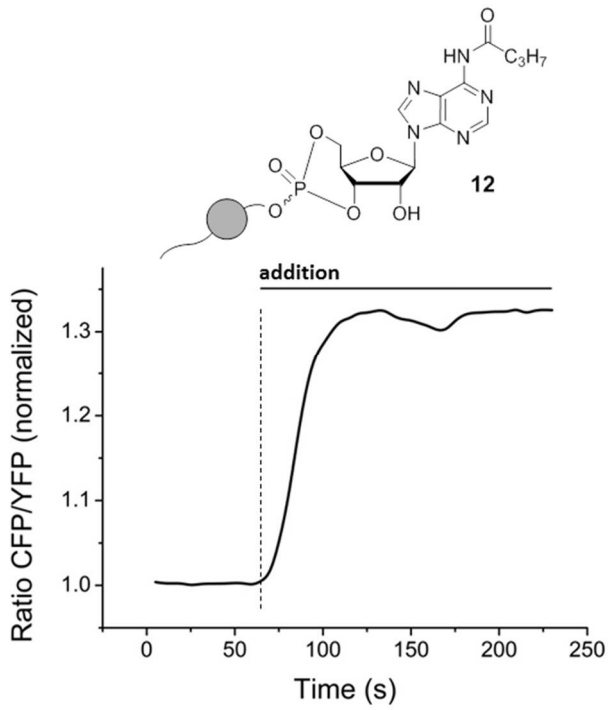

Figure 6: Normalized FRET ratio (between CFP and YFP) over the course of OB-N(Bu)-cAMP **12** addition to mouse cardiomyocytes Epac1-camps biosensor for intracellular cAMP. An instantaneous increase of FRET ratio after addition of **12** to the extracellular medium indicated intracellular release of cAMP and its binding to the FRET biosensor. Representative experiments (n=5).

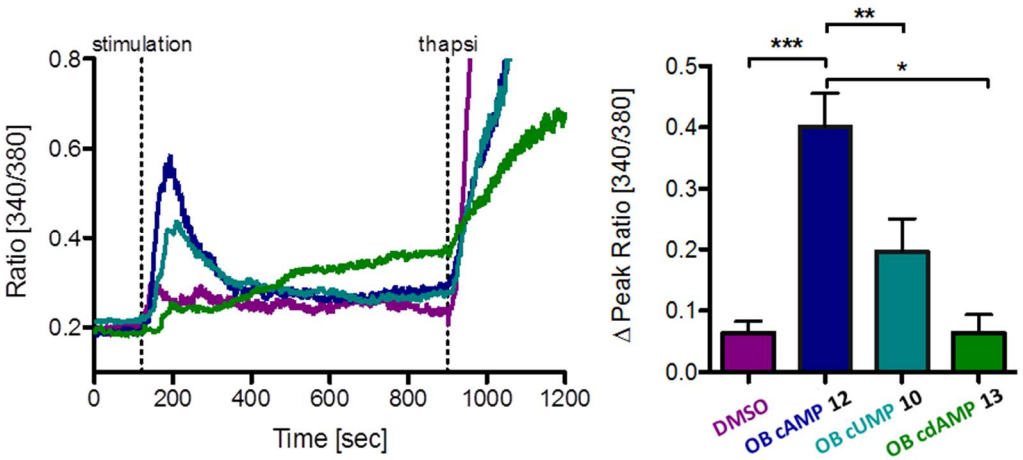

Figure 7: Stimulation of the of Jurkat T cells with OB-cNMPs **10,12** and **13**. Left: Jurkat T cells were stimulated after 120 s with the respective OB-cNMPs (20 µM) or DMSO (as negative control). Furthermore, as positive control Thapsigagarin (1.67 µM) was added after 900 s. Mean signal ratio between 340 nm and 380 nm from single cells are shown (DMSO n=26; OB cAMP n=77; OB cUMP n=37; OB cdAMP n=14). The addition of **12** and **10** resulted in a transient increase of the Ca^{2+} concentration, while no transient increase is visible for **13** or DMSO. Right: Statistical analysis of the mean delta peak for the OB-cNMPs and DMSO (data represent mean ± SEM). The most pronounced effect is measured for **12** and statistically significant differences between are marked by asterisks (* $p < 0.05$, ** $p<0.01$, *** $p<0.001$, Kruskal-Wallis Test).

The results confirmed again that the OB-masked cNMPs were able to cross the cell membrane and, importantly, immediately triggered cellular responses. In this context, it was concluded that

de-masked cNMPs promoted the observed effects based on the results of the previous hydrolysis studies and the substrate specify Ca^{2+} signaling events display.

The hydrolysis product of **12** acted as it would be expected for cAMP supporting the assumption that the N^6-butyryl group was either removed enzymatically, too, or that its presence did not impede receptor activation.

Comparison of the measured effects with those evoked by NH_2-unmodified OB-cAMP **15** and e.g. further nucleobase derivatives of adenosine or uridine in combination with incubation studies in cell homogenate could help to finalize the analysis and clarify whether the N^6-butyryl group is cleaved or the interacting receptors and binding sites lack selectivity in the corresponding region. Studies along these lines are currently performed in our laboratories.

In summary, the performed cell assays confirmed excellent membrane-permeability of the selected OB-cNMPs. Further, the cellular effects observed allow the conclusion that the bio-reversible protection at the phosphate was removed rapidly and efficiently. A fast enzymatic activation of the prepared OB-cNMPs was shown analogously in hydrolysis studies using pig liver esterase. The esterase cleaved the OB-mask even at low concentration within very short time, so that similar effects can be expected to proceed in cells. Finally, the observed FRET-sensor binding site interaction and induced Ca^{2+} mobilization proved that biologically active compounds were released out of the masked cNMPs. Moreover, the masked nucleotides triggered processes like they are attributed to their parent cNMPs (if existent in nature/identified yet).

3. Materials and Methods

All reactions involving water-sensitive reagents were conducted under anhydrous conditions and a dry atmosphere of nitrogen.

Reagents were used as purchased from commercial suppliers.

Anhydrous *N*,*N*-dimethylformamide (DMF) was purchased and stored over 4 Å molecular sieves.

All *other anhydrous solvents* were purified and dried using a solvent purification system (MB SPS-800 from Braun) and stored over appropriate molecular sieves.

Solvents for *normal phase* (NP) chromatography were distilled prior to use. Acetonitrile was purchased in HPLC grade for *reversed phase* (RP) chromatography and HPLC.

Evaporation of solvents was performed under reduced pressure on a rotary evaporator or using a high vacuum pump.

Reactions were monitored via *thin layer chromatography* (TLC) carried out on pre-coated Macherey-Nagel TLC plates Alugram® Xtra SIL G/UV_{254}, and compounds stained with Vanillin (Vanillin (5 g), 1000 mL MeOH/AcOH 9:1, 35 mL H_2SO_4) under heating.

For automated NP or RP chromatography two flash systems (Interchim Puriflash 430 or Sepacore® Flash System, combined with Chromabond® Flash RS 80 SiOH (NP) or RS40 C_{18} ec (RP) columns) were used. For purifications of phosphordiamidites, a chromatotron (Harrison Research 7924T) with glass plates coated with 2 or 4 mm layers of VWR60 PF_{254} silica gel containing a fluorescent indicator (VWR no. 7749) was used.

Analytical RP-*High Performance Liquid Chromatography-Mass Spectrometry* (RP-HPLC/MS) was performed with an Agilent 1260 Infinity instrument (pump G1311B, autosampler G1329B, column compartment G1316A, diode array detector G4221B, column Agilent Poroshell 120 EC-C18, 2.7 mm, 4.6x50 mm) coupled with single-quad MS (Advion expression^L CMS).

Ultrapure water was generated by a Sartorius Aurium® pro unit (Sartopore 0.2 µm, UV). As elution buffer served a tetra-*n*-butylammonium acetate solution (10 mM, pH 7.2). HPLC/MS runs were performed according to the following method: 0 – 15 min: water/acetonitrile gradient (2% – 98% B) with a flow of 0.5 mL/min, 20 °C column temperature and UV detection at 259 nm and 270 nm, MS scans from 150 to 1100 m/z.

Nuclear magnetic resonance (NMR) spectra were recorded at room temperature on Bruker Fourier 300 (300 MHz for ^1H acquisitions), Bruker AMX 400 (400 MHz for ^1H 101 MHz for ^{13}C and 152 MHz for ^{31}P acquisitions) or Bruker AVIII 600 (600 MHz for ^1H and 151 MHz for ^{13}C acquisitions) spectrometers in automation mode. All chemical shifts (δ) are given in parts per million (ppm) with

the solvent resonance as internal standard. Coupling constants *J* are given in Hertz (Hz). Two-dimensional NMR experiments (HSQC, HMBC) were used for the assignment of quaternary carbons.

For *mass spectrometric* (MS) analytic, spectra were acquired on an Agilent 6224 ESI-TOF spectrometer in positive and negative mode as required.

Infrared spectroscopy (IR) was carried out with a Bruker Alpha P FT-IR in attenuated total reflection (ATR) mode at room temperature ranging from 400 cm^{-1} to 4000 cm^{-1}.

For *FRET measurements*, primary mouse ventricular cardiomyocytes were isolated from Epac1-camps biosensor expressing transgenic mice[27] as described[26] and plated onto laminin coated glass cover slides. Measurements were performed 1 – 2 h after plating using a Nikon Ti microscope based FRET imaging system containing pE-100 440 nm light source (CoolLED), DV2 Dual View and ORCA-03G charge-coupled device camera (Hamamatsu), and analyzed as described[26]. Cells were kept in a buffer containing 144 mM NaCl, 5.4 mM KCl, 1 mM $MgSO_4$, 1 mM $CaCl_2$, 10 mM Hepes (pH 7.3) and stimulated with OB-cNMPs dissolved 1:1000 in the same buffer from a freshly made 20 mM DMSO stock solution.

For *Ca^{2+} mobilization assays*, Jurkat T cells were incubated with the membrane-permeable AM ester of the Ca^{2+} dye Fura-2 (4 µM, Calbiochem). Therefore, about 2 x 10^6 cells were centrifuged at 500 g for 5 min and resuspended in 1 mL of freshly supplemented RPMI medium containing Fura-2 AM. Cells were incubated for 30 min at 37 °C. After centrifugation, cells were washed and resuspended in Ca^{2+} buffer [140 mM NaCl, 5 mM KCl, 1 mM $MgSO_4$, 1 mM $CaCl_2$, 20 mM Hepes (pH 7.4), 1 mM NaH_2PO_4, 5 mM glucose] and kept for 20 min at room-temperature (RT) for de-esterification. Cells were added on prepared coverslips and allowed to adhere before measurement. Slides were mounted onto a Leica IRBE microscope (100-fold magnification) and after 120s the respective OB-cNMPs (20 µM) or DMSO (as control) were added. As positive control, Thapsigagarin (1.67 µM, Calbiochem) was added after 900 s. A Sutter DG-4 was used as a light source, and frames were acquired with an electron-multiplying charge-coupled device camera (C9100-13, Hamamatsu). Images (512 × 512 pixels) were acquired in 16-bit mode with the following filter sets (AHF Analysentechnik) [excitation (ex), beam splitter (bs), and emission (em), all in nanometers]: Fura-2 (ex, HC 340/26, HC 387/11; bs, 400DCLP; em, 510/84).

General Procedures:

GP I: *N*-butanoylation of nucleosides via transient TMS-protection:

The respective nucleoside (adenosine, guanosine or 2'-deoxyadenosine) was co-evaporated three times and then dissolved in anhydrous pyridine (2 – 5 mL/mmol), and diluted either with the same volume of THF or double the volume of CH_2Cl_2. At 0 °C, TMSCl (2.1 – 9.0 equiv.) was added. The reaction mixture was allowed to warm up to rt and stirred for 5 – 18 h. Successively, butyryl chloride (1.1 equiv.) was added slowly and the reaction mixture stirred for another 6 h at rt. Cleavage of TMS ethers was promoted by the addition of either 1 M HCl (0.5 mL/mmol) under vigorous stirring for 5 min, or methanol (2 - 5 mL/mmol) and stirring at rt for further 12 h. The reaction was terminated by removal of all volatile components under high vacuum. The crude residue was co-evaporated with toluene and CH_2Cl_2 several times, and then taken up in acetonitrile/demin. water. Purification was performed by means of automated RP flash column chromatography on C_{18} modified silica gel with an acetonitrile gradient in water (0% to 100%).

GP II: 3',5'-Phosphorylation of nucleosides to their OB-masked cNMP analogues:

Under an atmosphere of nitrogen, the respective nucleoside was dissolved in DMF/CH_3CN (25 mL/mmol). In a separate flask, bis(*N*,*N*-di*iso*propylamino)-4-octanoyloxybenzyl phosphor-amidite (1 equiv.) was dissolved in acetonitrile (25 mL/mmol total volume). The phosphor diamidite solution and DCI (0.25 M in CH_3CN, 1.3 – 1.5 equiv.) were added slowly and dropwise in five to ten portions to the nucleoside solution. The addition of more DCI (0.25 M in CH_3CN, 1.2 – 1.5 equiv.) or 5-(benzylthio)-1*H*-tetrazole (BTT, 0.3 M in CH_3CN, 1.3 equiv.) followed, and the reaction mixture was stirred 1 h further. Then, *t*BuOOH (5.5 M in *n*-decane, 1.5 equiv.) was added and the solution

stirred for 10 min more. Successively, all volatile components were removed in vacuum, and the obtained residue was taken up in CH_3CN/demin. water and purified by means of an automated RP flash column chromatography on C_{18} modified silica gel with an CH_3CN gradient in water (0% to 100%).

Syntheses:

Synthesis of bis(*N*,*N*-di*iso*propylamino)-4-octanoyloxybenzyl phosphordiamidite **3**:

1.00 g (3.75 mmol) bis(*N*,*N*-di*iso*propylamino)chlorophosphine **1** were dissolved in 15 mL anhydrous THF. In a separate flask, 0.68 mL (4.87 mmol, 1.3 equiv.) NEt_3 and 0.94 g (3.75 mmol, 1 equiv.) 4-(hydroxymethyl)phenyloctanoate **2** were mixed with 7 mL anhydrous THF, and the mixture was added dropwise to the chlorophosphine. The reaction mixture was stirred at rt for 20 h, then filtrated and the filtrate concentrated to dryness in vacuum. The remaining residue was purified by NP chromatography on silica gel with PE/TEA 98:2 as eluents, and the desired product obtained as colorless syrup.

Yield: 1.28 g (2.67 mmol, 71%).

^{1}H-NMR (600 MHz, chloroform-d): δ [ppm] = 7.36 (d, $^2J_{H,H}$ = 8.2 Hz, 2 H), 7.14 – 6.95 (m, 2 H), 4.63 (d, $^2J_{H,H}$ = 7.2 Hz, 2 H), 3.66 – 3.51 (m, 4 H), 2.54 (t, $^{2,3}J_{H,H}$ = 7.5 Hz, 2 H), 1.75 (p, $^{2,3}J_{H,H}$ = 7.4 Hz, 2 H), 1.51 – 1.23 (m, 8 H), 1.21 (d, $^2J_{H,H}$ = 2.7 Hz, 12 H), 1.20 (d, $^2J_{H,H}$ = 2.8 Hz, 12 H) 0.88 (t, $^{2,3}J_{H,H}$ = 7.3 Hz, 3 H).

^{13}C{^{1}H}-NMR (151 MHz, chloroform-d): δ [ppm] = 172.6, 149.7, 138.2, 127.9, 121.5, 65.8, 44.69, 44.56, 34.6, 31.8, 29.2, 29.1, 25.1, 24.8, 24.7, 24.1, 24.0, 22.75, 14.22.

^{31}P{^{1}H}-NMR (162 MHz, chloroform-d): δ [ppm] = 123.5.

IR (ATR): ṽ in [cm^{-1}] = 2963.3, 2927.8, 2861.4, 2079.0, 2025.5, 1761.3, 1607.8, 1507.4, 1457.5, 1416.5, 1390.1, 1361.6, 1300.3, 1194.2, 1184.8, 1162.9, 1140.3, 1116.2, 1045.2, 1016.9, 952.7, 916.5, 866.3, 779.6, 748.7, 706.7, 642.7, 566.1, 527.6.

MS (MALDI): m/z [M-H] calc. for $C_{27}H_{48}N_2O_3P^-$: 479.340, found: 479.245.

Synthesis of 6-*N*-butanoyl-adenosine **7**:

In accordance with GP I, 1.40 g (5.26 mmol) adenosine **4** were dissolve in 34 mL pyridine/THF 1:1 and converted with 2.11 mL (16.5 mmol, 3.2 equiv.) TMSCl and 0.60 mL (5.78 mmol, 1.1 equiv.) butyryl chloride. After 6 h stirring at rt, 2.5 mL 1 M HCl (aq.) was added to cleave the TMS ethers, and after 5 min, all volatile components were removed under vacuum. Upon final purification of the crude product via automated RP flash column chromatography on C_{18} modified silica gel with an CH_3CN gradient in water (0% to 100%), the product was obtained as colorless powder.

Yield: 1.09 g (3.22 mmol, 61%).

^{1}H-NMR (500 MHz, DMSO-d$_6$): δ [ppm] = 10.63 (s, 1 H), 8.69 (s, 1 H), 8.65 (s, 1 H), 6.01 (d, $^3J_{H,H}$ = 5.8 Hz, 1 H), 5.53 (d, $^3J_{H,H}$ = 5.8 Hz, 1 H), 5.23 (d, $^3J_{H,H}$ = 4.8 Hz, 1 H), 5.12 (t, $^3J_{H,H}$ = 5.6 Hz, 1 H), 4.63 (q, $^3J_{H,H}$ = 5.4 Hz, 1 H), 4.19 (q, $^3J_{H,H}$ = 4.3 Hz, 1 H), 3.98 (q, $^3J_{H,H}$ = 3.9 Hz, 1 H), 3.76 – 3.64 (m, 1 H), 3.58 (ddd, $^2J_{H,H}$ = 11.9 Hz, $^3J_{H,H}$ = 6.1 Hz, $^3J_{H,H}$ = 4.0 Hz, 1 H), 2.55 (t, $^{2,3}J_{H,H}$ = 7.3 Hz, 2 H), 1.63 (h, $^{2,3}J_{H,H}$ = 7.4 Hz, 2 H), 0.94 (t, $^{2,3}J_{H,H}$ = 7.4 Hz, 3 H).

^{13}C-NMR (126 MHz, DMSO-d$_6$): δ [ppm] = 171.5, 151.7, 151.6, 149.7, 142.7, 123.9, 87.6, 85.7, 73.7, 70.3, 61.3, 38.0, 18.2, 13.5.

IR (ATR): ṽ in [cm^{-1}] = 3273.2, 2963.3, 2934.0, 2875.0, 1716.3, 1685.0, 1613.3, 1587.0, 1521.9, 1460.3, 1409.0, 1356.6, 1327.0, 1224.3, 1124.1, 1082.2, 1056.7, 984.6, 902.4, 866.3, 799.6, 745.0, 704.7, 643.7, 547.3.

MS (ESI-HR): m/z [M+H]$^+$ calc. for $C_{14}H_{20}N_5O_5^+$: 338.1459, found: 338.1469.

Synthesis of 6-*N*-butanoyl-2'-deoxyadenosine **8**:

Following GP I, 1.14 g (4.24 mmol) 2'-deoxyadenosine **5** were dissolve in 24 mL pyridine/CH_2Cl_2 1:2. At 0 °C, 1.13 mL (8.91 mmol, 2.1 equiv.) TMSCl were added, and the reaction mixture was stirred for 18 h at rt. Successively, 0.48 mL (4.67 mmol, 1.1 equiv.) butyryl chloride were added. After further 3 h stirring at rt, the TMS ethers were removed by addition of 8 mL CH_3OH at 0 °C. After further 5 h at rt, the reaction was terminated by removing all volatile components under

vacuum. The crude product was taken up in water containing little amount of CH_3CN and purified via automated RP flash column chromatography on C_{18} modified silica gel with an CH_3CN gradient in water (0% to 100%) to afford the desired product as colorless powder.

Yield: 0.43 g (1.35 mmol, 32%).

^{1}H-NMR (400 MHz, methanol-d$_4$): δ [ppm] = 8.66 (s, 1 H), 8.62 (s, 1 H), 6.61 – 6.52 (m, 1 H), 4.64 (dt, $^3J_{H,H}$ = 6.1 Hz, $^3J_{H,H}$ = 3.1 Hz, 1 H), 4.10 (q, $^3J_{H,H}$ = 3.4 Hz, 1 H), 3.88 (dd, $^2J_{H,H}$ = 12.2 Hz, $^3J_{H,H}$ = 3.4 Hz, 1 H), 3.79 (dd, $^2J_{H,H}$ = 12.2 Hz, $^3J_{H,H}$ = 3.9 Hz, 1 H), 2.88 (ddd, $^2J_{H,H}$ = 13.4 Hz, $^3J_{H,H}$ = 7.4 Hz, $^3J_{H,H}$ = 6.0 Hz, 1 H), 2.67 (t, $^{2,3}J_{H,H}$ = 7.4 Hz, 2 H), 2.51 (ddd, $^2J_{H,H}$ = 13.5 Hz, $^3J_{H,H}$ = 6.2 Hz, $^3J_{H,H}$ = 3.3 Hz, 1 H), 1.82 (h, $^{2,3}J_{H,H}$ = 7.4 Hz, 2 H), 1.08 (t, $^{2,3}J_{H,H}$ = 7.4 Hz, 3 H).

^{13}C{^{1}H}-NMR (101 MHz, methanol-d$_4$): δ [ppm] = 174.4, 152.9, 150.7, 144.3, 123.2, 89.7, 86.7, 72.7, 63.4, 41.5, 39.9, 19.6, 14.0.

IR (ATR): ṽ in [cm^{-1}] = 3336.8, 2964.6, 2933.1, 2875.3, 2592.1, 2330.9, 1682.2, 1612.5.1585.9, 1522.5, 1459.6, 1402.8, 1354.8, 1329.2, 1223.8, 1093.3, 1058.5, 993.8, 941.1, 867.1, 799.6, 749.6, 984.8, 644.4, 585.3, 561.2, 542.4, 527.4, 509.6, 464.7.

MS (ESI-HR): m/z [M+H]$^+$ calc. for $C_{14}H_{20}N_5O_4^+$: 322.1510, found: 322.1521.

Synthesis of 2-*N*-butanoyl-guanosine **9**:

According to GP I, 1.55 g (5.48 mmol) guanosine **6** were co-evaporated with pyridine three times and then dissolved in 81 mL pyridine/CH_2Cl_2 1:2. At 0 °C, 6.28 mL (49.4 mmol, 9 equiv.) TMSCl were added, and the reaction mixture was stirred for 4 h at rt. Successively, 0.62 mL (6.03 mmol, 1.1 equiv.) butyryl chloride were added. After 3 h stirring at rt, the cleavage of the TMS ethers was induced by addition of 27 mL CH_3OH, and after further 12 h at rt, the reaction was terminated and all volatile components were removed under vacuum. The crude residue was taken up in water containing little amount of CH_3CN and finally purified via automated RP flash column chromatography on C_{18} modified silica gel with an CH_3CN gradient in water (0% to 100%) to afford the desired product as colorless powder.

Yield: 0.92 g (2.61 mmol, 48%).

^{1}H-NMR (400 MHz, DMSO-d$_6$): δ [ppm] = 12.07 (bs, 1 H), 11.71 (bs, 1 H), 8.26 (s, 1 H), 5.80 (d, $^3J_{H,H}$ = 5.7 Hz, 1 H), 5.47 (d, $^3J_{H,H}$ = 5.7 Hz, 1 H), 5.17 (d, $^3J_{H,H}$ = 4.5 Hz, 1 H), 5.03 (t, $^3J_{H,H}$ = 5.4 Hz, 1 H), 4.43 (d, $^3J_{H,H}$ = 5.2 Hz, 1 H), 4.20 – 4.05 (m, 1 H), 3.90 (q, *J* = 3.9 Hz, 1 H), 3.64 (dt, $^2J_{H,H}$ = 11.9 Hz, $^3J_{H,H}$ = 4.8 Hz, 1 H), 3.55 (dt, $^2J_{H,H}$ = 11.9 Hz, $^3J_{H,H}$ = 4.7 Hz, 1 H), 2.45 (t, $^{2,3}J_{H,H}$ = 7.3 Hz, 2 H), 1.62 (h, $^{2,3}J_{H,H}$ = 7.4 Hz, 2 H), 0.92 (t, $^{2,3}J_{H,H}$ = 7.5 Hz, 3 H).

^{13}C{^{1}H}-NMR (101 MHz, DMSO-d$_6$): δ [ppm] = 176.2, 154.8, 148.8, 148.0, 137.6, 120.1, 86.6, 85.3, 73.9, 61.1, 37.8, 17.9, 13.4.

IR (ATR): ṽ in [cm^{-1}] = 3364.4, 3279.5, 2968.3, 2941.1, 1680.2, 1608.8, 1564.3, 1554.1, 1536.0, 1481.4, 1469.2, 1449.9, 1402.5, 1251.7, 1204.2, 1179.4, 1127.9, 1089.0, 1060.2, 993.3, 976.4, 901.1, 863.3, 818.6, 801.0, 762.7, 737.4, 717.0, 680.4, 643.7, 607.0, 589.1, 562.3, 510.2, 484.2.

MS (ESI-HR): m/z [M+H]$^+$ calc. for $C_{14}H_{19}N_5O_6^+$: 354.1408, found: 354.1400.

Synthesis of uridine-3',5'-(4-octanoyloxybenzyl)cyclophosphate **10**:

According to GP II, 26 mg (0.11 mmol) uridine **10** were dissolved in 2 mL DMF and reacted with 57 mg (0.12 mmol, 1.1 equiv.) OB-PA_2 **3**, dissolved in 2.5 mL CH_3CN, in the presence of 0.54 mL (0.13 mmol, 1.3 equiv.) DCI (0.25 M in CH_3CN) and 0.45 mL (0.13 mmol, 1.3 equiv.) BTT (0.3 M in CH_3CN). The addition of 32 µL (0.16 mmol, 1.5 equiv.) *t*BuOOH (5.5 M in *n*-decane) followed successively. After purification by automated RP flash column chromatography on C_{18} modified silica gel with a CH_3CN gradient in water (0% to 100%) and lyophilization, the product was obtained as colorless cotton and in two fractions containing each of the stereoisomers.

Yield: 11 mg (0.02 mmol, 19%).

^{1}H-NMR (400 MHz, methanol-d$_4$): δ [ppm] = 7.66 – 7.51 (m, 2 H), 7.47 (d, $^3J_{H,H}$ = 8.1 Hz, 1 H), 7.22 – 7.08 (m, 2 H), 5.69 (d, $^3J_{H,H}$ = 8.0 Hz, 1 H), 5.64 (d, $^3J_{H,H}$ = 0.9 Hz, 1 H), 5.24 – 5.14 (m, 2 H), 4.64 (ddd, $^3J_{H,P}$ = 22.5 Hz, $^2J_{H,H}$ = 9.3 Hz, $^3J_{H,H}$ = 4.6 Hz, 1 H), 4.39 (ddd, $^3J_{H,H}$ = 10.2, $^2J_{H,H}$ = 9.4, $^3J_{H,H}$ = 0.8 Hz, 1 H),

4.35 – 4.25 (m, 2 H), 4.25 – 4.10 (m, 1 H), 2.58 (t, $^{2,3}J_{H,H}$ = 7.4 Hz, 2 H), 1.73 (p, $^{2,3}J_{H,H}$ = 7.4 Hz, 2 H), 1.53 – 1.22 (m, 8 H), 1.05 – 0.82 (m, 3 H)

and

7.63 (d, $^{3}J_{H,H}$ = 8.1 Hz, 1 H), 7.53 – 7.47 (m, 2 H), 7.19 – 7.10 (m, 2 H), 5.73 (d, $^{3}J_{H,H}$ = 1.2 Hz, 1 H), 5.71 (d, $^{3}J_{H,H}$ = 8.1 Hz, 1 H), 5.19 (d, $^{2}J_{H,H}$ = 8.7 Hz, 2 H), 4.81 (ddd, $^{3}J_{H,P}$ = 9.8 Hz, $^{3}J_{H,H}$ = 5.1 Hz, $^{3}J_{H,H}$ = 1.0 Hz, 1 H), 4.67 (ddd, $^{3}J_{H,P}$ = 14.2 Hz, $^{2}J_{H,H}$ = 9.2 Hz, $^{3}J_{H,H}$ = 5.5 Hz, 1 H), 4.62 – 4.47 (m, 2 H), 4.42 (td, $^{2}J_{H,H}$ = 10.1, $^{3}J_{H,H}$ = 5.5 Hz, 1 H), 2.60 (t, $^{2,3}J_{H,H}$ 7.4 Hz, 2 H), 1.74 (p, $^{2,3}J_{H,H}$ 7.4 Hz, 2 H), 1.50 – 1.26 (m, 8 H), 1.02 – 0.84 (m, 3 H).

$^{13}C\{^{1}H\}$-NMR (101 MHz, methanol-d_4): δ [ppm] = · 173.8, 165.9, 151.5, 150.1, 143.7, 134.3, 131.2, 123.3, 103.0, 97.5, 80.1, 72.4, 71.5, 71.2, 70.3, 35.0, 32.9, 30.2, 30.1, 25.0, 23.7, 14.4

and

172.8, 164.9, 151.7, 150.5, 143.5, 133.0, 130.2, 122.8, 103.1, 97.7, 79.3, 72.4, 71.2, 71.1, 70.6, 35.0, 32.8, 30.2, 30.1, 26.0, 23.7, 14.4.

$^{31}P\{^{1}H\}$-NMR (162 MHz, methanol-d_4): δ [ppm] = --3.93, -5.01.

MS (ESI-HR): m/z $[M+Na]^+$ calc. for $C_{24}H_{31}N_2O_{10}PNa^+$: 561.1609, found: 561.1445.

Synthesis of 6-*N*-butanoyl-adenosine-3',5'-(4-octanoyloxybenzyl)cyclophosphate **12**:

According to GP II, 48 mg (0.14 mmol) 6-*N*-butanoyl-adenosine **7** were dissolved in 4 mL DMF and treated with a solution of 76 mg (0.16 mmol, 1.1 equiv.) OB-PA_2 **3** in 4 mL CH_3CN and 0.97 mL (0.24 mmol, 1.7 equiv.) DCI (0.25 M in CH_3CN) as well as 0.62 mL (0.19 mmol, 1.3 equiv.) BTT (0.3 M in CH_3CN). Then, 43 µL (0.21 mmol, 1.5 equiv.) *t*BuOOH (5.5 M in *n*-decane) were added. After purification by automated RP flash chromatography on C_{18} modified silica with a CH_3CN gradient in water (0% to 100%), the product was obtained as colorless cotton and mixture of two diastereomers.

Yield: 13 g (0.02 mmol, 14%).

^{1}H-NMR (400 MHz, methanol-d_4): δ [ppm] = 8.68, 8.58 (2 x s, 2 H), 8.49, 8.38 (2x s, 2 H), 7.62 – 7.56, 7.55 – 7.49 (2 x m, 4 H), 7.17 – 7.12, 7.13 – 7.06 (2 x m, 4 H), 6.20, 6.12 (2 x s, 2 H), 5.47 (dd, $^{3}J_{H,P}$ = 9.1 Hz, $^{3}J_{H,H}$ = 5.1 Hz, 1 H) 5.23 (2 x d, $^{2}J_{H,H}$ = 10.4 Hz & 8.1 Hz, 4 H), 5.05 (ddd, $^{3}J_{H,P}$ = 9.6 Hz, $^{3}J_{H,H}$ = 5.1 Hz, $^{3}J_{H,H}$ = 1.6 Hz, 1 H), 4.89 – 4.86 (m, 1 H), 4.73 – 4.34 (m, 7 H), 2.71 – 2.55 (m, 6 H,), 2.51 (t, $^{2,3}J_{H,H}$ = 7.4 Hz, 2 H), 1.86 – 1.70 (m, 6 H), 1.68 – 1.57 (m, 2 H), 1.53 – 1.25 (m, 16 H), 1.05 (2 x t, $^{2,3}J_{H,H}$ = 7.4 Hz, 6 H), 0.98 – 0.95 (m, 6 H).

$^{13}C\{^{1}H\}$-NMR (151 MHz, methanol-d_4): δ [ppm] = 173.8, 173.6, 152.8, 152.4, 150.8, 143.1, 133.3, 133.2, 130.7, 130.6, 124.5, 123.1, 123.0, 88.8, 81.7, 80.4, 69.3, 69.2, 68.5, 59.8, 39.9, 34.5, 31.8, 29.2, 29.1, 25.0, 22.8, 18.5,14.2, 13.9.

$^{31}P\{^{1}H\}$-NMR (162 MHz, methanol-d_4): δ [ppm] = -3.80, -4.90.

MS (ESI-HR): m/z $[M+H]^+$ calc. for $C_{29}H_{39}N_5O_9P^+$: 632.2848, found: 632.2848.

Synthesis of 6-*N*-butanoyl-2'-deoxyadenosine-3',5'-(4-octanoyloxybenzyl)cyclophosphate **13**:

According to GP II, 50 mg (0.15 mmol) 6-*N*-butanoyl-2'-deoxyadenosine **8** were dissolved in 4 mL DMF and reacted with 82 mg (0.17 mmol, 1.1 equiv.) OB-PA_2 **3**, dissolved in 4.3 mL CH_3CN, in the presence of 1.60 mL (0.40 mmol, 2.6 equiv.) DCI (0.25 M in CH_3CN) in total and 50 µL (0.25 mmol, 1.6 equiv.) *t*BuOOH (5.5 M in *n*-decane). After purification by automated RP flash column chromatography on C_{18} modified silica gel with a CH_3CN gradient in water (0% to 100%) and lyophilization, the product was obtained as colorless cotton and mixture of two diastereomers.

Yield: 12 mg (0.02 mmol, 13%).

^{1}H-NMR (400 MHz, methanol-d_4): δ [ppm] = 8.69 (s, 1 H), 8.61 (s, 1 H), 8.47 (s, 1 H), 8.37 (s, 1 H), 7.65 – 7.57, 7.55 – 7.48 (2 x m, 2 H), 7.19 – 7.10 (m, 4 H), 6.59 (dd, $^{3}J_{H,H}$ = 9.0 Hz, $^{3}J_{H,H}$ = 2.0 Hz, 1 H), 6.55 (dd, $^{3}J_{H,H}$ = 6.7 Hz, $^{3}J_{H,H}$ = 4.0 Hz, 1 H), 5.64 (q, $^{3}J_{H,H/P}$ = 9.2 Hz, 1 H), 5.33 (q, $^{3}J_{H,H/P}$ = 9.2 Hz, 1 H), 5.23 (2 x d, $^{2}J_{H,H}$ = 13.1 Hz & $^{3}J_{H,H}$ = 12.9 Hz, 4 H), 4.70 – 4.40 (m, 4 H), 4.22 (td, $^{3}J_{H,H}$ = 9.9 Hz, $^{3}J_{H,H}$ = 5.6 Hz, 1 H), 4.08 (td, $^{3}J_{H,H}$ = 9.9 Hz, $^{3}J_{H,H}$ = 4.7 Hz, 1 H), 2.98 (ddd, $^{2}J_{H,H}$ = 13.1 Hz, $^{3}J_{H,H}$ = 7.7 Hz, $^{3}J_{H,H}$ = 1.9 Hz, 1 H), 2.83 – 2.70 (m, 3 H), 2.69 – 2.57 (m, 6 H), 2.54 (t, $^{2,3}J_{H,H}$ = 7.4 Hz, 2 H), 1.90 – 1.70 (m, 6 H), 1.66 (q, $^{2,3}J_{H,H}$ = 7.3 Hz, 2 H), 1.51 – 1.26 (m, 16 H), 1.06 (2 x t, $^{2,3}J_{H,H}$ = 7.4, 6 H), 0.98 – 0.86 (m, 6 H).

$^{13}C\{^1H\}$-NMR (101 MHz, methanol-d_4): δ [ppm] = 174.5, 174.4, 173.8, 173.6, 153.4, 153.2, 152.8, 152.7, 152.4, 152.3, 150.8, 150.7, 144.6, 144.5, 134.4, 134.3, 131.1, 130.7, 123.2, 123.1, 122.6, 85.8, 85.6, 79.3, 79.2, 75.7, 75.6, 71.7, 71.6, 71.4, 71.3, 40.0, 39.9, 35.0, 34.9, 32.8, 30.1, 30.0, 25.9, 25.9, 23.7, 19.7, 19.6, 14.4, 14.1, 14.0.

$^{31}P\{^1H\}$-NMR (162 MHz, methanol-d_4): δ [ppm] = -4.14, -5.50.

MS (ESI-HR): m/z $[M+H]^+$ calc. for $C_{29}H_{39}N_5O_8P^+$: 616.2531, found: 616.2534.

Synthesis of 2-*N*-butanoyl-guanosine-3',5'-(4-octanoyloxybenzyl)cyclophosphate **14**:

In accordance with GP II, 52 mg (0.15 mmol) 6-*N*-butanoyl-guanosine **9** were dissolved in 4 mL DMF and treated with a solution of 77 mg (0.16 mmol, 1.1 equiv.) OB-PA_2 **3** in 4 mL CH_3CN, 1.75 mL (0.44 mmol, 3 equiv.) DCI (0.25 M in CH_3CN) in total and finally, 44 µL (0.21 mmol, 1.5 equiv.) *t*BuOOH (5.5 M in *n*-decane). After purification by automated RP flash column chromatography on C_{18} modified silica gel with a CH_3CN gradient in water (0% to 100%) and lyophilization, the product was obtained as colorless cotton and a single diastereomer.

Yield: 4 mg (5.6 µmol, 4%).

^1H-NMR (400 MHz, methanol-d_4): δ [ppm] = 7.92 (s, 1 H), 7.56 (d, $^3J_{H,H}$ = 8.2 Hz, 2 H), 7.07 (d, $^3J_{H,H}$ = 8.3 Hz, 2 H), 6.01 (s, 1 H), 5.23 (d, $^2J_{H,H}$ = 11.6 Hz, 2 H), 4.69 (ddd, $^3J_{H,H}$ = 22.2 Hz, $^3J_{H,P}$ = 9.4 Hz, $^3J_{H,H}$ = 4.8 Hz, 1 H), 4.55 (t, $^3J_{H,H}$ = 10.0 Hz, 1 H), 4.35 (dd, $^3J_{H,H}$ = 10.0 Hz, $^3J_{H,H}$ = 4.8 Hz, 1 H), 4.32 (d, $^3J_{H,H}$ = 4.7 Hz, 1 H), 4.18 (dd, $^3J_{H,P}$ = 9.9 Hz, $^3J_{H,H}$ = 4.7 Hz, 1 H), 2.51 (t, $^{2,3}J_{H,H}$ = 7.4 Hz, 2 H), 2.46 (t, $^{2,3}J_{H,H}$ = 7.1 Hz, 2 H), 1.74 (h, $^{2,3}J_{H,H}$ = 7.4 Hz, 2 H), 1.62 (t, $^{2,3}J_{H,H}$ = 7.1 Hz, 2 H), 1.49 – 1.25 (m, 8 H,), 1.02 (t, $^{2,3}J_{H,H}$ = 7.4 Hz, 3 H), 0.98 – 0.86 (m, 3 H).

$^{13}C\{^1H\}$-NMR (101 MHz, methanol-d_4): δ [ppm] = 177.7, 173.6, 152.2, 150.0, 149.8, 137.5, 134.4, 131.4, 123.3, 120.2, 93.4, 80.3, 73.3, 71.6, 71.5, 70.5, 39.4, 34.8, 32.9, 30.1, 25.8, 23.7, 19.3, 14.4, 13.9.

$^{31}P\{^1H\}$-NMR (162 MHz, methanol-d_4): δ [ppm] = --4.93.

MS (ESI-HR): m/z $[M+H]^+$ calc. for $C_{29}H_{39}N_5O_{10}P^+$: 648.2429, found: 648.2720.

Synthesis of adenosine-3',5'-(4-octanoyloxybenzyl)cyclophosphate **15**:

Following GP II, 21 mg (78 µmol) adenosine were dissolved in 2 mL DMF and treated with a solution of 41 mg (85 µmol, 1.1 equiv.) (OB)PA_2 **101** in 2 mL CH_3CN as well as 0.74 mL (0.19 mmol, 2.4 equiv.) DCI (0.25 M in CH_3CN). Lastly, 23 µL (0.12 mmol, 1.5 equiv.) *t*BuOOH (5.5 M in *n*-decane) were added for oxidation. After purification by automated RP flash column chromatography on C_{18} modified silica gel with a CH_3CN gradient in water (0% to 100%) and lyophilization, the product was obtained as a colorless cotton and mixture of two diastereomers.

Yield: 5 mg (10 µmol, 12%).

^1H-NMR (400 MHz, acetonitrile-d_3): δ [ppm] = 8.19 (s, 1 H), 8.09 (s, 1 H), 7.93 (s, 1 H), 7.88 (s, 1 H), 7.55 – 7.46 (m, 2 H), 7.45 – 7.41 (m, 2 H), 7.12 – 7.02 (m, 4 H), 5.99 (bs, 4 H), 5.98 (s, 1 H), 5.93 (s, 1 H), 5.47 (dd, $^3J_{H,P}$ = 9.1 Hz, $^3J_{H,H}$ = 5.1 Hz, 1 H), 5.27 (ddd, $^3J_{H,P}$ = 9.4 Hz, $^3J_{H,H}$ = 4.9 Hz, $^3J_{H,H}$ = 1.0 Hz, 1 H), 5.19 (ddd, $^3J_{H,P}$ = 9.3 Hz, $^3J_{H,H}$ = 5.0 Hz, $^3J_{H,H}$ = 1.6 Hz, 1 H), 5.14 – 5.06 (m, 4 H), 4.72 (d, $^3J_{H,H}$ = 4.9 Hz, 1 H), 4.60 (d, $^3J_{H,H}$ = 5.1 Hz, 1 H), 4.58 – 4.14 (m, 6 H), 2.50 (2 x t, $^3J_{H,H}$ = 7.5 Hz, 4 H), 1.64 (h, $^3J_{H,H}$ = 7.6 Hz, 4 H), 1.47 – 1.14 (m, 16 H), 0.89 – 0.78 (m, 6 H).

$^{13}C\{^1H\}$-NMR (151 MHz, acetonitrile-d_3): δ [ppm] = 173.3, 156.9, 153.9, 151.3, 149.4, 140.9, 133.3, 130.6, 130.7, 123.1, 119.8, 93.6, 81.0, 72.7, 71.5, 69.4, 34.7, 32.4, 29.6, 25.5, 23.3, 20.1, 14.3.

$^{31}P\{^1H\}$-NMR (162 MHz, acetonitrile-d_3): δ [ppm] = -4.37, -6.03.

MS (ESI-HR): m/z $[M+H]^+$ calc. for $C_{25}H_{33}N_5O_8P^+$: 562.2061, found: 562.2068.

4. Conclusions

In sum, we have identified an individually adaptable synthesis approach towards membrane-permeable, bio-reversibly masked cNMPs and prepared OB-cNMPs that fulfilled all requirements in terms of synthetic flexibility of the approach, chemical stability and enzymatic activation to be valuable new tools for the setup of novel cellular assays.

Author Contributions: conceptualization, A.R.; methodology, A.R., B.D., A.K. & V.N.; formal analysis, A.R.; investigation, A.R., B.D., A.K. & V.N.; resources, C.M.; writing—original draft preparation, A.R.;

writing—review and editing, A.R., B.D., A.G. & C.M.; project administration, A.R., B.D. & C.M.; funding acquisition, A.G. & C.M.

Funding: This research was funded by the Universität Hamburg and the Deutsche Forschungsgemeinschaft (DFG), grant number SFB1328.

Acknowledgments: E.M. is grateful for a fellowship by Advanced School C. Urbani, University of Camerino.

Conflicts of Interest: The authors declare no conflict of interest.

References

1. Seifert, R. Distinct Signaling Roles of cIMP, cCMP, and cUMP. *Structure* **2016**, *24*, 1627–1628, doi:10.1016/j.str.2016.09.002.

2. Zimmerman, A. L. *Cyclic nucleotide-gated ion channels*; Fourth Edi.; Elsevier Inc., 2012; ISBN 9780123877383.

3. Biel, M. *Cyclic nucleotide-regulated cation channels*; Second Edi.; Elsevier Inc., 2010; Vol. 2; ISBN 9780123741455.

4. Walsh, D. A.; van Patten, S. M. Multiple pathways signal transduction by the cAMP-dependent protein kinase. *FASEB J.* **1994**, *8*, 1227–1236.

5. Bopp, T.; Becker, C.; Klein, M.; Klein-Heßling, S.; Palmetshofer, A.; Serfling, E.; Heib, V.; Becker, M.; Kubach, J.; Schmitt, S.; Stoll, S.; Schild, H.; Staege, M. S.; Stassen, M.; Jonuleit, H.; Schmitt, E. Cyclic adenosine monophosphate is a key component of regulatory T cell–mediated suppression. *J. Exp. Med.* **2007**, *204*, 1303–1310, doi:10.1084/jem.20062129.

6. Bodor, J.; Bopp, T.; Vaeth, M.; Klein, M.; Serfling, E.; Hünig, T.; Becker, C.; Schild, H.; Schmitt, E. Cyclic AMP underpins suppression by regulatory T cells. *Eur. J. Immunol.* **2012**, *42*, 1375–1384, doi:10.1002/eji.201141578.

7. Wolf, I. M. A.; Diercks, B. P.; Gattkowski, E.; Czarniak, F.; Kempski, J.; Werner, R.; Schetelig, D.; Mittrücker, H. W.; Schumacher, V.; Von Osten, M.; Lodygin, D.; Flügel, A.; Fliegert, R.; Guse, A. H. Frontrunners of T cell activation: Initial, localized Ca2+ signals mediated by NAADP and the type 1 ryanodine receptor. *Sci. Signal.* **2015**, *8*, 1–13, doi:10.1126/scisignal.aab0863.

8. Engels, J.; Schlaeger, E. J. Synthesis, structure, and reactivity of adenosine cyclic 3′,5′-phosphate-benzyltriesters. *J. Med. Chem.* **1977**, *20*, 907–911, doi:10.1021/jm00217a008.

9. Korth, M.; Engels, J. The Effects of Adenosine- and Guanosine 3′,5′-Phosphoric Acid Benzyl Esters on Guinea-Pig Ventricular Myocardium. *Naunyn-Schmiedberg's Arch. Pharmacol.* **1979**, *314*, 103–111.

10. Schultz, C.; Vajanaphanich, M.; Harootunian, A. T.; Sammak, P. J.; Barrett, K. E.; Tsien, R. Y. Acetoxymethyl esters of phosphates, enhancement of the permeability and potency of cAMP. *J. Biol. Chem.* **1993**, *268*, 6316–6322.

11. Schultz, C.; Vajanaphanich, M.; Genieser, H. G.; Jastorff, B.; Barrett, K. E.; Tsien, R. Y. Membrane-permeant derivatives of cyclic AMP optimized for high potency, prolonged activity, or

690 rapid reversibility. *Mol. Pharmacol.* **1994**, *46*, 702–8.

691 12. Beckert, U.; Grundmann, M.; Wolter, S.; Schwede, F.; Rehmann, H.; Kaever, V.; Kostenis, E.; Seifert, R.
692 CNMP-AMs mimic and dissect bacterial nucleotidyl cyclase toxin effects. *Biochem. Biophys. Res.*
693 *Commun.* **2014**, *451*, 497–502, doi:10.1016/j.bbrc.2014.07.134.

694 13. Meier, C. Nucleoside diphosphate and triphosphate prodrugs – An unsolvable task? *Antivir. Chem.*
695 *Chemother.* **2017**, *25*, 69–82, doi:10.1177/2040206617738656.

696 14. Gollnest, T.; De Oliveira, T. D.; Rath, A.; Hauber, I.; Schols, D.; Balzarini, J.; Meier, C.
697 Membrane-permeable Triphosphate Prodrugs of Nucleoside Analogues. *Angew. Chemie - Int. Ed.* **2016**,
698 *55*, 5255–5258, doi:10.1002/anie.201511808.

699 15. Meier, C.; Jessen, H. J.; Schulz, T.; Weinschenk, L.; Pertenbreiter, F.; Balzarini, J. Rational Development
700 of Nucleoside Diphosphate Prodrugs: DiPPro-Compounds. *Curr. Med. Chem.* **2015**, *22*, 3933–3950,
701 doi:10.2174/0929867322666150825163119.

702 16. Thomson, W.; Nicholls, D.; Irwin, W. J.; Al-Mushadani, J. S.; Freeman, S.; Karpas, A.; Petrik, J.;
703 Mahmood, N.; Hay, A. J. Synthesis, bioactivation and anti-HIV activity of the bis(4-acyloxybenzyl) and
704 mono(4-acyloxybenzyl) esters of the 5′-monophosphate of AZT. *J. Chem. Soc. Perkin Trans. 1* **1993**, 1239–
705 1245, doi:10.1039/P19930001239.

706 17. Mitchell, A. G.; Thornson, W.; Nicholls, D.; Irwin, W. J.; Freeman, S. Bioreversible Protection for the
707 Phospho Group: Bioactivation of the Di (4-acyloxybenzyl) and Mono(4-acyloxybenryl) P hosp hoesters
708 of Methyl phosphonate and Phosphonoacetate. *J. Chem. Soc. Perkin Trans. 1* **1992**, *3*, 2345–2353.

709 18. Pahnke, K.; Meier, C. Synthesis of a Bioreversibly Masked Lipophilic Adenosine Diphosphate Ribose
710 Derivative. *ChemBioChem* **2017**, *18*, 1616–1626, doi:10.1002/cbic.201700232.

711 19. Gollnest, T.; De Oliveira, T. D.; Schols, D.; Balzarini, J.; Meier, C. Lipophilic prodrugs of nucleoside
712 triphosphates as biochemical probes and potential antivirals. *Nat. Commun.* **2015**, *6*, 1–15,
713 doi:10.1038/ncomms9716.

714 20. Jessen, H. J.; Schulz, T.; Balzarini, J.; Meier, C. Bioreversible protection of nucleoside diphosphates.
715 *Angew. Chemie - Int. Ed.* **2008**, *47*, 8719–8722, doi:10.1002/anie.200803100.

716 21. Schulz, T.; Balzarini, J.; Meier, C. The DiPPro approach: Synthesis, hydrolysis, and antiviral activity of
717 lipophilic d4T diphosphate prodrugs. *ChemMedChem* **2014**, *9*, 762–775, doi:10.1002/cmdc.201300500.

718 22. Weinschenk, L.; Schols, D.; Balzarini, J.; Meier, C. Nucleoside Diphosphate Prodrugs: Nonsymmetric
719 DiPPro-Nucleotides. *J. Med. Chem.* **2015**, *58*, 6114–6130, doi:10.1021/acs.jmedchem.5b00737.

720 23. Fan, Y.; Gaffney, B. L.; Jones, R. A. Transient silylation of the guanosine O6 and amino groups facilitates
721 N-acylation. *Org. Lett.* **2004**, *6*, 2555–2557, doi:10.1021/ol049096i.

722 24. Dahl, B. H.; Nielsen, J.; Dahl, O. Mechanistic studies on the phosphoramidite coupling reaction in
723 oligonucleotide synthesis. I. Evidence for nudeophilic catalysis by tetrazole and rate variations with the

phosphorus substituents. *Nucleic Acids Res.* **1987**, *15*, 1729–1743, doi:10.1093/nar/15.4.1729.

25. Russell, M. A.; Laws, A. P.; Atherton, J. H.; Page, M. I. The mechanism of the phosphoramidite synthesis of polynucleotides. *Org. Biomol. Chem.* **2008**, *6*, 3270–3275, doi:10.1039/b808999j.

26. Börner, S.; Schwede, F.; Schlipp, A.; Berisha, F.; Calebiro, D.; Lohse, M. J.; Nikolaev, V. O. FRET measurements of intracellular cAMP concentrations and cAMP analog permeability in intact cells. *Nat. Protoc.* **2011**, *6*, 427–438, doi:10.1038/nprot.2010.198.

27. Calebiro, D.; Nikolaev, V. O.; Gagliani, M. C.; De Filippis, T.; Dees, C.; Tacchetti, C.; Persani, L.; Lohse, M. J. Persistent cAMP-signals triggered by internalized G-protein-coupled receptors. *PLoS Biol.* **2009**, *7*, doi:10.1371/journal.pbio.1000172.